Final technical report for Phenomic Analysis of Natural and Induced Variation in Brachypodium Distachyon DE-SC0001526

Abstract

The goal of this project was to apply high-throughput, non-destructive phenotyping (phenomics) to collections of natural variants and induced mutants of the model grass *Brachypodium distachyon* and characterize a small subset of that material in detail. *B. distachyon* is well suited to this phenomic approach because its small size and rapid generation time allow researchers to grow many plants under carefully controlled conditions. In addition, the simple diploid genetics, high quality genome sequence and existence of numerous experimental tools available for *B. distachyon* allow us to rapidly identify genes affecting specific phenotypes. Our phenomic analysis revealed great diversity in biofuel-relevant traits like growth rate, biomass and photosynthetic rate. This clearly demonstrated the feasibility of applying a phenomic approach to the model grass *B. distachyon*. We also demonstrated the utility of *B. distachyon* for studying mature root system, something that is virtually impossible to do with biomass crops. We showed tremendous natural variation in root architecture that can potentially be used to design crops with superior nutrient and water harvesting capability. Finally, we demonstrated the speed with which we can link specific genes to specific phenotypes by studying two mutants in detail. Importantly, in both cases, the specific biological lessons learned were grass-specific and could not have been learned from a dicot model system. Furthermore, one of the genes affects cell wall integrity and thus may be a useful target in the context of biomass crop improvement. Ultimately, all this information can be used to accelerate the creation of improved biomass crops, but this was beyond the scope of this project.

Accomplishments

Our results can be broken into four areas: 1) selecting and creating the collections of plants to be phenotyped; 2) establishing phenomic methods for *B. distachyon*; 3) phenotypic characterization of the germplasm collections; 4) detailed genetic characterization of a select group of mutants.

1) Selecting and creating the collections of plants to be phenotyped

For this project we used two complementary sources of variation: diverse natural accessions collected from a broad geographic area and T-DNA mutants that contained a randomly inserted piece of DNA. Through prior work we had assembled a collection of 187 natural accessions and used SSR markers to show that this collection contained considerable genetic variation. One complicating factor is that flowering time varies considerably among these accessions. One group in particular requires a very long period of vernalization (>6 weeks) to induce flowering. Thus, we chose to focus on 100 lines with more modest vernalization requirements (4 weeks or less) to allow meaningful comparisons between lines.

Through another DOE-funded grant we created a collection of T-DNA mutants and by using the know sequence of the T-DNA as a handle we sequenced a small segment of DNA flanking the insertion site. This allowed us to identify the insertion site and determine if the insertion disrupts a gene. For this project, we selected T-DNA lines with insertions in or very close to genes. However, before we could phenotype them we needed to make them homozygous. To do this we grew up several individuals from each line and used PCR to identify homozygous lines (Fig.1). Homozygosity was confirmed in the next generation. In total, we created 600 homozygous lines. At the time, we were limited by the number of available T-DNA lines with insertions in genes. In addition to being used for this project, the homozygous lines are being distributed to researchers who request specific mutants.

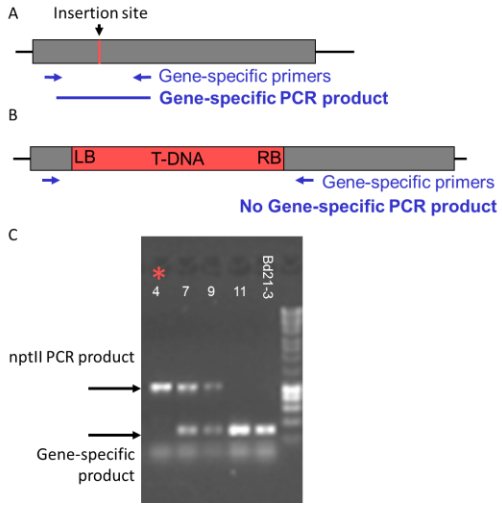

Figure 1. Identification of homozygous T-DNA lines by multiplex PCR. PCR using DNA primers flanking the insertion site will produce a product when a wild-type copy of the gene is present (A) but no PCR product is produced in lines homozygous for the T-DNA insertion (B). (C) An image of a gel showing that line 4, highlighted by *, lacks the gene specific PCR product and is thus homozygous for an insertion at this site. The nptII PCR product is only present in lines that contain a T-DNA insert. This band in sample 4 confirms the presence of template DNA. PCR reactions from plants that are not homozygous yield both products or only the gene-specific product.

2) Establishing phenomic methods for *B. distachyon*

Prior to phenoptying the entire collections, we optimized several growth parameters by growing a smaller number of accessions under different day lengths, nutrient levels and light levels. The first parameters we examined were vernalization, daylength and light levels. Since flowering time has a huge effect on biomass we wanted to identify conditions under which all the natural accessions flowered at approximately the same time. To do this we staggered the vernalization such that some lines were incubated in the cold for more time than other lines, but all lines were removed from the cold at the same time. Since the lines grow very little in the cold, they were all essentially the same size when placed in the warm growth chamber. By testing a subset of diverse lines we found that 4 weeks of vernalization for most lines and 1 week for the most rapid flowering lines resulted in nearly synchronous flowering for all lines (Fig. 2) These results were published in Tyler et al. 2014.

From previous work we know that long days could accelerate flowering and overcome the vernalization requirement for some lines. Thus, our initial starting conditions were 20 hour light:4 hr dark light cycle at a light intensity of 150 µmol m^{-2} s^{-1}. While these conditions

promoted rapid flowering, we wanted to further optimize light conditions. We tested 3 different day lengths with line Bd21-3, our standard wild-type and the line from which all the T-DNA lines originated. We noted that plants grown under 16 hour days were more robust and still flowered in a reasonable amount of time (Fig 3A). Thus, we conducted subsequent experiments under 16 hour days. We also determined photosynthetic rates for 12 natural accessions under several light intensities. Interestingly, we observed a 3-fold variation in photosynthetic rates indicating large natural variation in this important trait. We also observed that *B. distachyon* can use more light than our standard conditions so we increased the light level for subsequent experiments to 800 µmol m^{-2} s^{-1}(Fig 3B). For the bulk of our phenotyping we wanted to use levels of nitrogen and phosphorus that were limiting but not deficient for plant growth. We reasoned that such levels would allow us to identify lines that were better at nutrient use efficiency. To select the appropriate levels we determined the effect of varying nitrogen and phosphorus levels on a handful of natural accessions. As expected, plant growth was limited under very low N and P levels (Fig. 4). Interestingly, by using repeated non-destructive imaging we could calculate the relative growth rates from one week to the next. We observed that some lines tended to grow more rapidly earlier while others grew more rapidly later (Fig. 4). We also examined chlorophyll content and photosynthetic efficiency and observed that low P levels decreased photosynthetic efficiency while low N levels did not (Fig. 5). Both low N and P levels decreased chlorophyll content (Fig. 5). These and more results on N and P utilization were published in Poire et al. 2014.

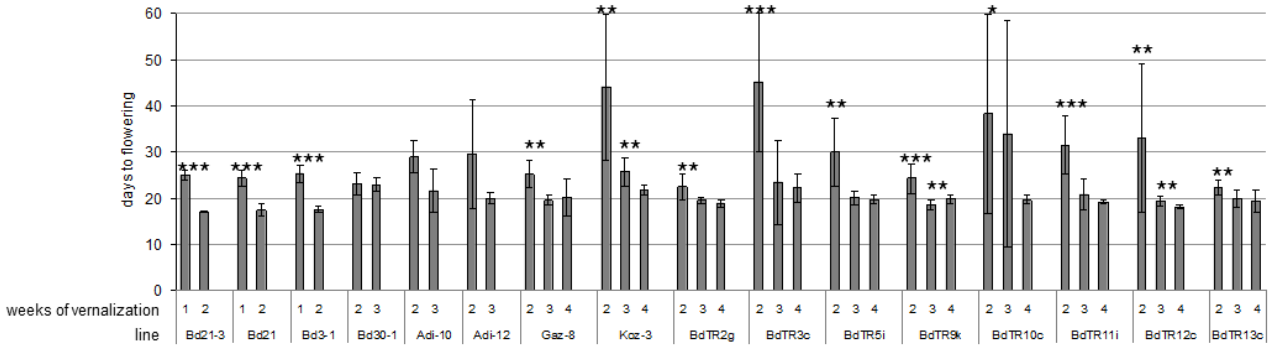

Figure 2. Flowering time responsiveness to vernalization. Seeds of inbred lines were cold-treated for the number of weeks indicated on the x-axis. Seeds were all sown on the same day and then grown under a 20-hour photoperiod. Flowering time was recorded for each plant when the first flower was visible to the naked eye. For calculation purposes, plants that had not yet flowered by the end of the experiment, 81 days after transfer to the growth chamber, were recorded as having a flowering time of 81 days. The average flowering time (y-axis) for each line and cold treatment is shown. Error bars indicate the standard deviation based on 13-20 plants. To test the statistical significance of observed differences, pairwise ANOVAs were performed for the longest cold treatment compared to each of the shorter cold treatments for each line. *: **p**-value < 0.05, **: **p**-value < 0.01, ***: **p**-value < 0.001. From Tyler et al. 2014.

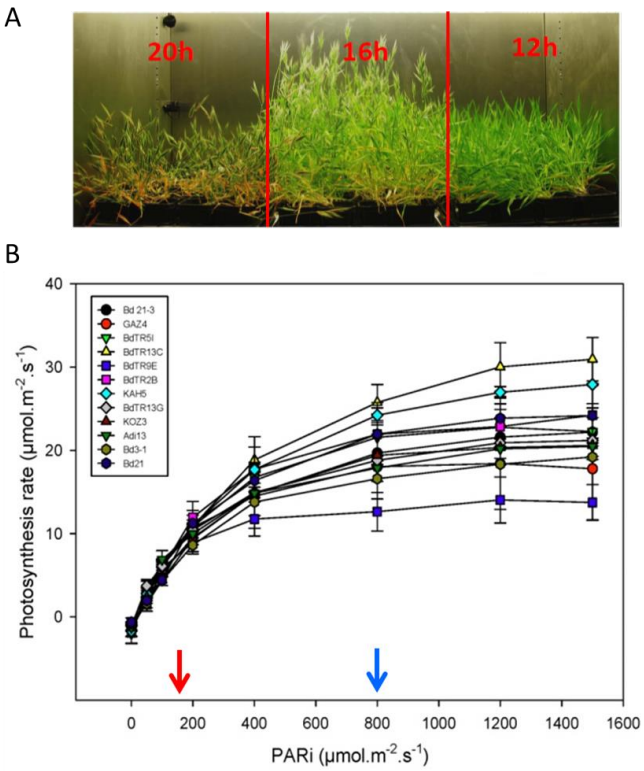

Figure 3. Light optimization. (A) Line Bd21-3 was grown under different day lengths. Note that plants grown under 16hr days were healthiest. (B) To select the optimal light intensity for growing *B. distachyon* we measured the photosynthetic rates of 12 natural accessions under different light intensities. The plants were initially grown at 200 µmol m^{-2} s^{-1} and then subjected to the light intensities indicated to measure photosynthetic rate. Note that photosyntehic rate begins to plateau at 800 µmol m^{-2} s^{-1}, considerably higher than the 150 µmol m^{-2} s^{-1} (red arrow) that we routinely grew *B. distachyon* under. This indicates that while *B. distachyon* can tolerate lower light levels it can utilize much more light. This adaptability is one reason that *B. distachyon* is easy to grow. We conducted subsequent experiments at 800 µmol m^{-2} s^{-1} indicated by the blue arrow. Note that the final photosynthetic rate varies more than 3 fold among these accessions.

3) Phenotypic characterization of the germplasm collections

After optimizing growth conditions, we phenotyped the full collection of natural accessions and T-DNA lines. As expected, we observed considerable variation in all parameters for the natural accessions. Examples of this variation are shown in figure 6.

In addition to above ground parameters we also examined root system size and architecture and how those traits varied in response to different N, P and soil moisture levels. In most grasses, including all biomass crops and grains, the root system is composed of roots originating from three different places. Primary root(s) originate from the embryo during germination, coleoptile nodal roots originate from the coleoptile and leaf nodal roots originate from stem nodes (Fig. 7; Poiré, et al. 2014. Significantly, these different root types may respond to drought differently and seem to function differently for nutrient uptake. Thus, an understanding of the genetic mechanisms controlling roots system architecture would be useful for identifying breeding targets for biomass crops. We examined root system architecture in 79 accessions and observed considerable variation (Table 1; Fig. 7).

To begin the process of identifying the genetic basis of the variation observed we phenotyped a population of recombinant inbred lines (RILs) developed from a cross between two inbred lines. Interestingly, while these lines had similar biomass their progeny were much more variable (Fig. 8A). Such transgressive segregation suggests that several alleles at different loci affect this trait. This is supported by a QTL analysis indicating the presence of three strong QTLs that together explain 59% of the variance (Fig. 8).

For the T-DNA lines, we expect a different pattern of variation than is observed for diverse natural accessions. Since each T-DNA line only contains a mutation(s) in one or a few genes we expect that most mutations will not have a large effect on any given phenotype. Thus, for any particular measurement we expect to see most of the lines appear wild-type and very few to deviate significantly. Figure 9 shows examples of this expected phenotypic distribution.

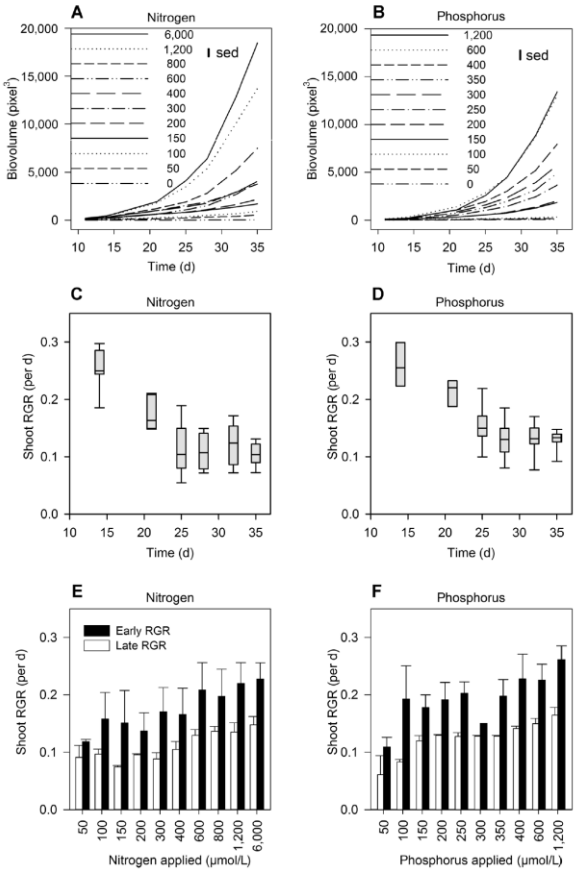

Figure 4. Biomass and relative growth rate (RGR) in response to N and P treatments

Biovolume over 5 weeks of growth for Bd21‐3 at various N (A) and P (B) nutrition rates. RGR values calculated for N between 100 and 6,000 mmol/L (C) and P between 100 and 1,200 mmol/L (D) over time (box plot). Average RGR is indicated by a solid line. Relative Growth Rate values of Bd21‐3 at various N (E) and P (F) concentrations. Split RGR values subsequently calculated for early exponential growth phase (black bars) and late linear growth phase (white bars). Error bars are standard error of the difference for panels A and B. Error bars represent the standard error of means in panels E and F. (from Poiré et al. 2014)

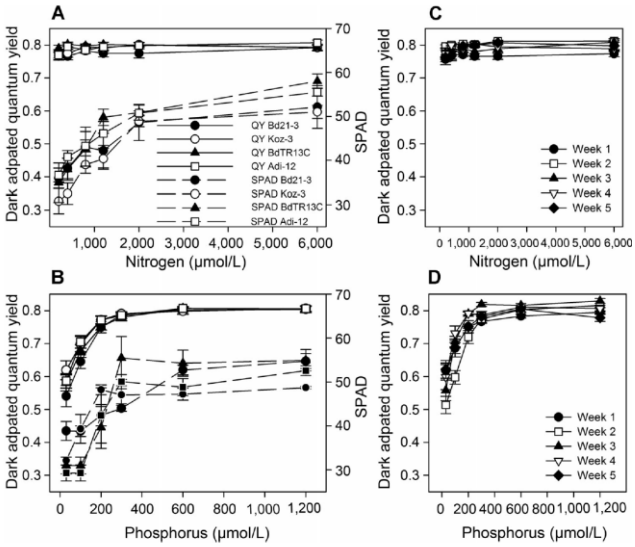

Figure 5. Dark-adapted quantum yield and SPAD. (A, B) Dark-adapted quantum yield showing the photochemical efficiency of the photosystem II (solid lines) and SPAD values (dashed lines) of four genotypes at various N (A) or P (B) concentrations. Data of 5 weeks of measurements are averaged. Error bars represent the standard error of means of four biological replicates over 5 weeks (20 points). Dark-adapted quantum yield showing the photochemical efficiency of the photosystem II averaged for all genotypes every week for N (C) and P (D) treatments. Data of 5 weeks of measurements are superimposed to illustrate the robustness of the observation over time.

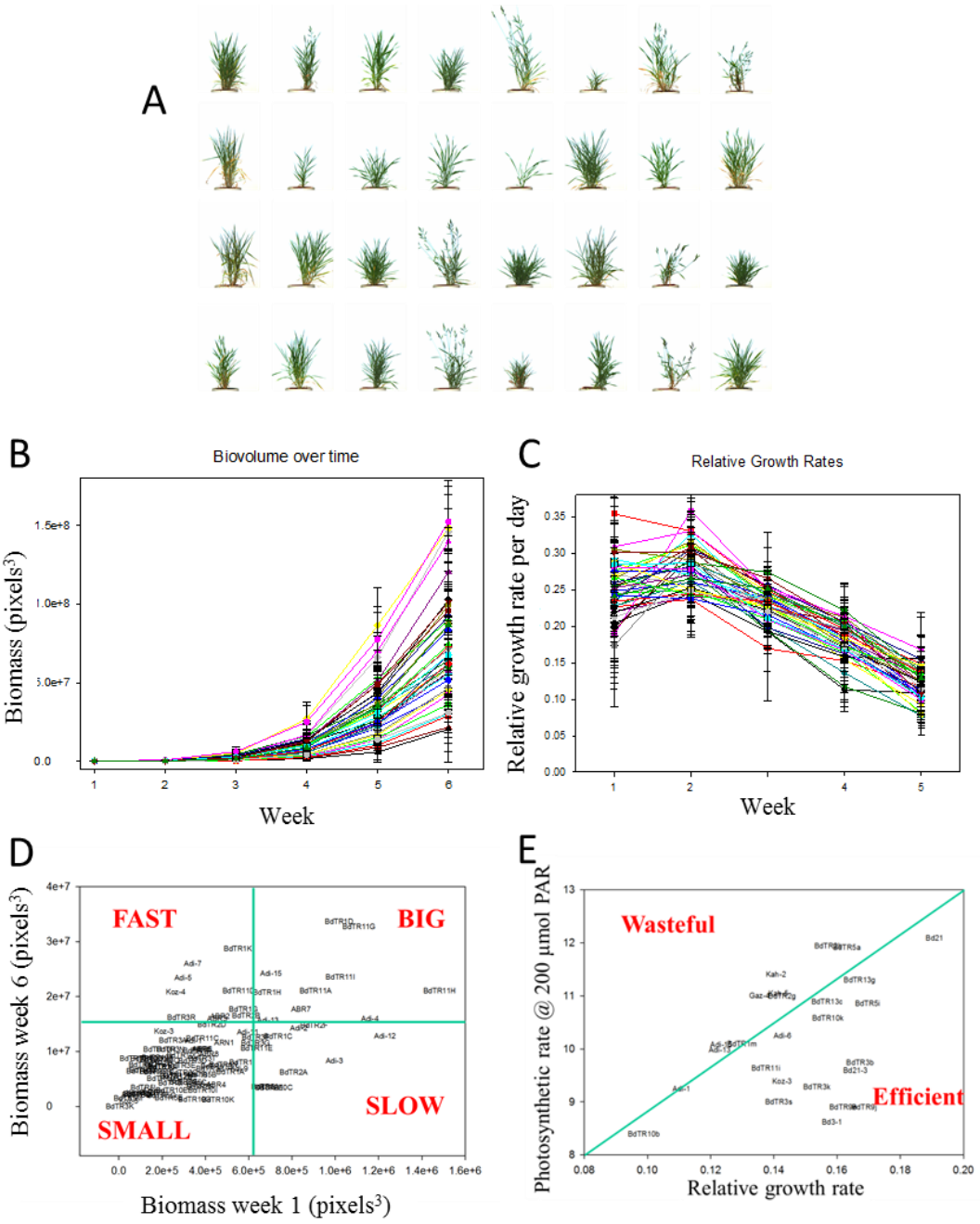

Figure 6. Phenotypic variation among natural accessions. (A) Visual appearance of 32 accessions. (B) Biomass over time for 48 accessions. Note the over 10-fold variation in biomass. (C) Relative growth rates were calculated by comparing the biomass of each individual plant to the previous week. Note the over 2-fold variation in relative growth rate. (D) By plotting early biomass vs late biomass we can see different growth strategies. For example, some lines are always big or small whereas a few lines start small but finish large or vice versa. (E) By plotting relative growth rate vs. photosynthetic rate we can that some lines appear to more efficiently convert photosynthate into biomass.

Table 1. Range of variation observed in root phenotypes among 36 *B. distachyon* accessions in one experiment or for 79 accessions in multiple experiments.

	Phenotype measured	**All experiments (79 lines)**	**One experiment (36 lines)**
Whole plant	Total dry weight (mg)	88.6 to 773.8 (*x8.7*)	285.6 to 438 (*x1.5*)
Total root system	Total root length (m)	1050 to 10770 (*x10.3)*	2090 to 5140 (*x2.5)*
	Root dry weight (mg)	28.9 to 312.17(*x10.8)*	62.2 to 179.1(*x2.9)*
	% of TDW in root system	20.5 to 60.6 *(x3)*	20.5 to 44.3 *(x2.2)*
	Root dry weight to shoot dry wt ratio	0.26 to 1.54 (*x6*)	0.26 to 0.80 (*x3.1*)
Primary seminal roots (PSR)	PSR partitioning (% of TRL)	14.9 to 94.1 (*x6.3)*	31.3 to 72.3 (*x2.3)*
	Number of PSR axile roots	1	1
	Branch roots (cm.(cm of axile root)$^{-1}$)	19.9 to 109.3*(x5.5)*	29.3 to 104.3 *(x3.6)*
Coleoptile nodal roots (CNR)	CNR partitioning (% of TRL)	0 to 57.1	0 to 49.8
	Number of CNR axile roots	0 to 2	0 to 2
	Branch roots (cm.(cm of axile root)$^{-1}$)	0 to 77.8	0 to 77.8
Leaf nodal roots (LNR)	LNR partitioning (% TRL)	4.2 to 72.7 (*x17.5)*	6 to 64.8 (*x10.9)*
	Number of LNR axile roots	2 to 22.2 *(x11.1)*	3.3 to 15.3 *(x4.6)*
	Branch roots (cm.(cm of axile root)$^{-1}$)	2.1 to 25.4 *(x12.1)*	3.2 to 15.9 *(x5)*

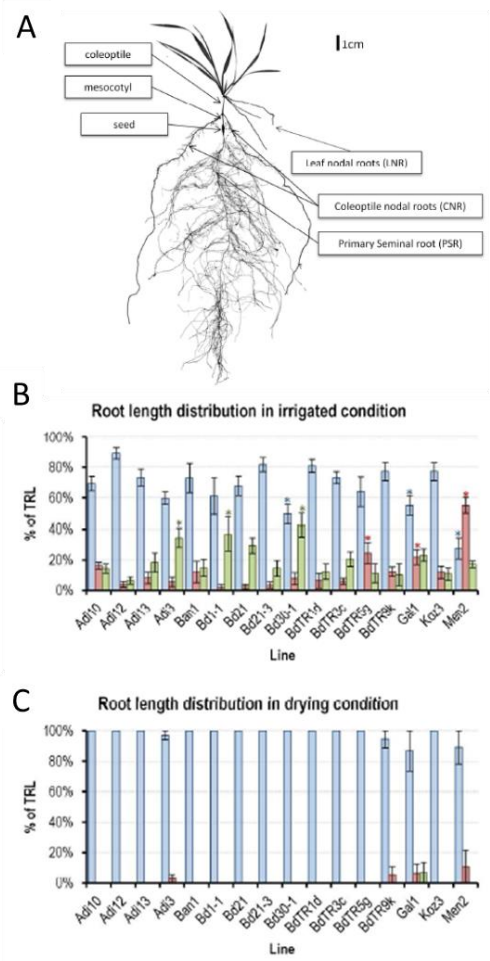

Figure 7. Example of roots system variation. (A) *Brachypodium distachyon* plant scanned at the fourth leaf stage, with root and shoot phenotypes studied indicated. The Distribution of the total root length among the three root types in 16 lines in irrigated (B) and in drying soil profile (B). Percentage of total root length in PSR (blue), CNR (red), and LNR (green). Error bars represent the standard errors based on four replicates. Asterisks show significant differences with Bd21-3 ($p<0.05$).

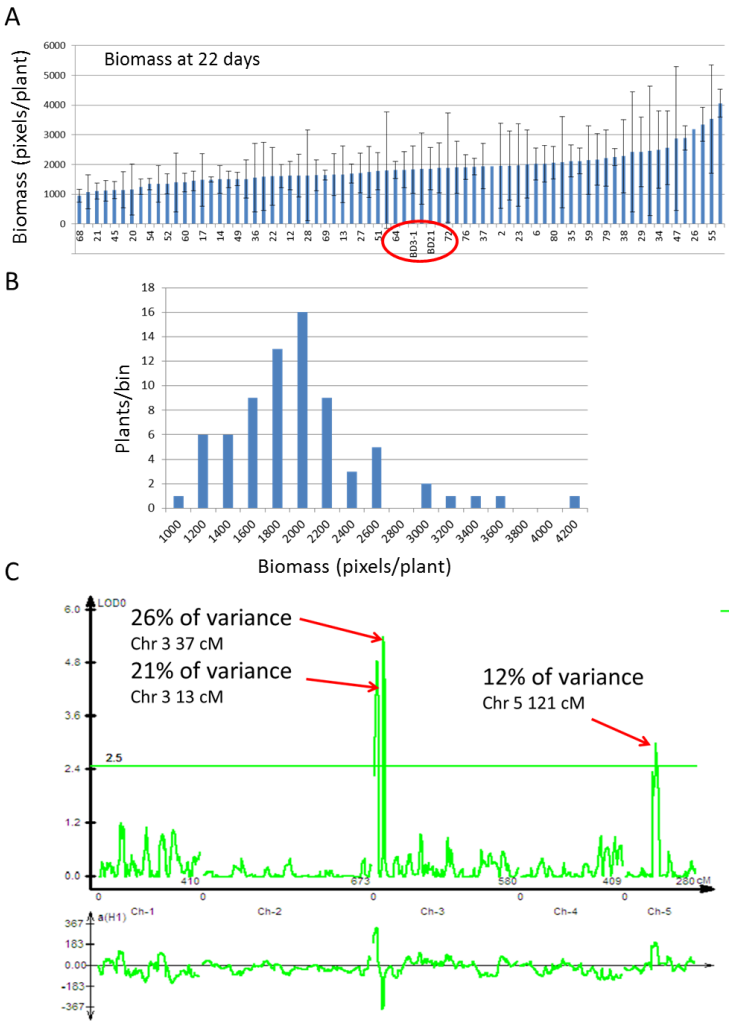

Figure 8. QTL analysis. (A) Biomass at 22 days for 72 RILs. Note that the parents of the cross (circled in red) have a similar biomass, but that the progeny exhibit a much greater diversity in biomass. (B) Lines grouped according to biomass ranges. Note the tail of higher biomass lines. (C) QTL analysis indicating the presence of three major QTLs contributing to biomass at 22 days.

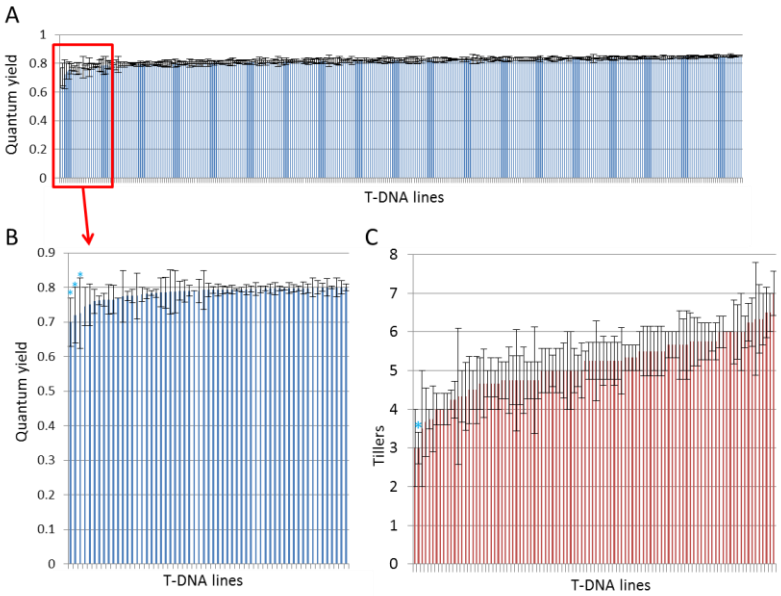

Figure 9. Phenotyping T-DNA lines. (A) Photosynthetic rate of 340 homozygous T-DNA lines. Note that most lines appear wild-type. (B) The tail of the graph in (A). Note that the three lines on the left designated by * have low photosynthetic rates and have been chosen for follow up experiments. (C) Tiller number for 100 T-DNA lines. The line marked by and * has retested for the low tiller phenotype. The other lines have not been retested.

4) Detailed genetic characterization of two select mutants.

We selected two mutants with clear morphological defects for detailed analysis (Figs. 10 and 11). In both cases we demonstrated that the T-DNA insertion co-segregated with the phenotype and showed that the phenotypes were recessive. This suggests that the phenotype is due to a loss of function mutation caused by the insertion of the T-DNA into the genes defined by our sequencing of DNA flanking the insertion sites. To definitively demonstrate that the loss of function of the candidate genes is responsible for the observed phenotype we complemented both mutants by introducing a wild-type copy of the gene. In both cases, the wild-type gene complemented the mutation and restored a wild-type phenotype (Fig. 12). Thus, we have fully demonstrated the utility of the T-DNA collection.

We named one of the mutants *crackle 1* (*crk1*) because mutant leaves were very brittle and often broke when handled or cracked when simply growing (Fig 11). This phenotype indicates that *crk1* decreases cell wall strength compromising the strength of the plant. The *CRK1* gene, Bradi3g34531, is similar to 4-Coumarate-CoA Ligase (4CL) a gene known to play a role in the biosynthesis of lignin monomers. However, it does not belong to the group of true 4CL genes and thus may not play a direct role in lignin biosynthesis. In addition to brittle leaves the *crk1* mutation causes developmental defects including flower development. Surprisingly, despite the severe floral defects, the mutant occasionally sets a few viable seeds. These seeds give rise to homozygous mutant plants indicating that some *crk1* flowers are fully fertile.

The second mutant we characterized in detail is named *bushy 1* (*bsh1*) because the most obvious phenotype is the large number of tillers and short stature of the plants (Fig. 11). Unlike *crk1*, *bsh1* plants make normal looking flowers. However, despite possessing normal-looking flowers, *bsh1* plants are completely sterile. We stained *bsh1* pollen with a modified

Figure 10 The *crk1* phenotype. Four week old wild type (A) and *crk1* (B) plants. Wild type (C) *crk1* (D) leaves at three magnifications. (E-H) Wild type flowers. (I) Wild type anther stained with Alexander's stain. (J-M) *crk1* flowers. Note that the flower in (L) is a rare normal-looking flower. (N) *crk1* anther stained with Alexander's stain. Note the presence of viable red pollen grains. (C-F) Unlabeled scale bars 1mm.

Alexander's stain to determine its viability. Virtually all pollen stained appeared misshapen and non-viable (Fig. 10). We pollinated *bsh1* flowers with wild-type pollen and those flowers set seed that gave rise to heterozygous offspring. Taken together, these results indicate that the *BSH1* gene is required for male fertility and normal development.

A major reason for studying *B. distachyon* is to learn about unique aspects of grass biology. Thus, we were interested in determining if *BSH1* and *CRK1* play the same role in the dicot *Arabidopsis thaliana*. To accomplish this we first identified the *A. thaliana* orthologs using BLAST and comparative genomics of the flanking regions. For both genes we were able to identify a single orthologous gene in *A. thaliana*. Fortunately, there are multiple *A. thaliana* T-DNA lines with insertions in these genes. We genotyped these lines and observed no obvious phenotype in the homozygous mutants (Fig 12 C and D). Thus, either these genes serve different functions in *B. distachyon* and *A. thaliana* or there is some sort of functional redundancy present in *A. thaliana*. In either case, we have gained knowledge about the unique biology of a grass that could not be learned without studying a grass model system.

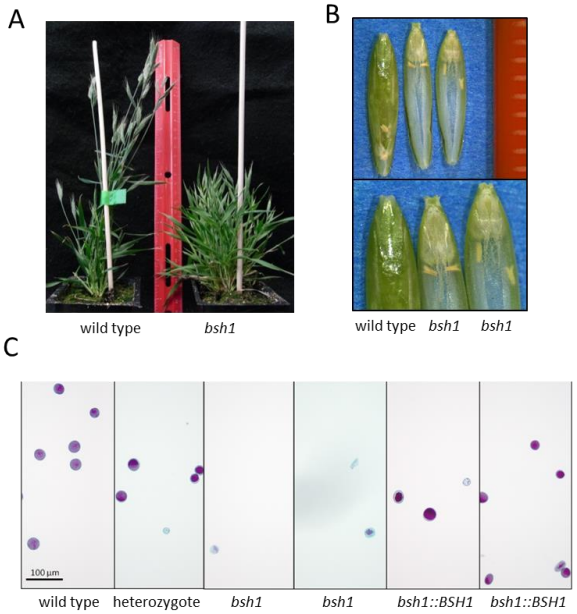

Figure 11. The *bsh1* phenotype. (A) Mature wild type and *bsh1* plants. (B) Wild type and bsh1 flowers/seeds. Note that the wild-type seed has grown considerably pushing up the old anthers whereas bsh1 flowers are infertile. (C) Modified Alexander staining of pollen to determine viability. Viable pollen stains purple.

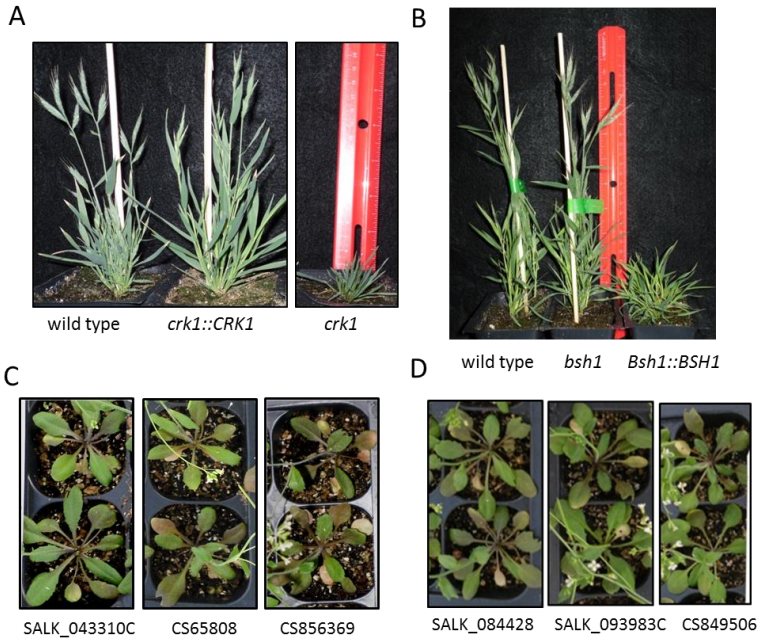

Figure 12. Complementation and grass-specificity of *CRK1* and *BSH1*. (A) Transformation of *crk1* with a wild-type version of the *CRK1* gene rescues the *crk1* phenotype. (B) Transformation of the *bsh1* with a wild-type version of the *BSH1* gene rescues the *bsh1* phenotype. Mutations in the Arabidopsis orthologs of *CRK1* (C) and *BSH1* (D) genes have no obvious phenotypes.

Conclusion

We demonstrated the feasibility of applying a phenomic approach to the model grass *B. distachyon*. The phenotyping work revealed great diversity in biofuel-relevant traits like growth rate, biomass and photosynthetic rate. We also demonstrated the utility of *B. distachyon* for studying mature root system, something that is virtually impossible to do with biomass crops. We showed tremendous natural variation in root architecture that can potentially be used to design crops with superior nutrient and water harvesting capability. Finally, we demonstrated the speed with which we can link specific genes to specific phenotypes by studying two mutants in detail. Importantly, in both cases, the specific biological lessons learned were grass-specific and could not have been learned from a dicot model system. Furthermore, one of the genes affects cell wall integrity and thus may be a useful target in the context of biomass crop improvement.

Training

Four post-doctoral fellows, one Ph.D. student and one student intern students worked on this project.

Publications and impact

Publications (7)

Chochois, V., Vogel, J., Rebetzke, G., Watt, M. 2014 Variation in adult plant phenotypes and partitioning among seed and stem-borne roots across 79 *Brachypodium distachyon* accessions to exploit in breeding cereals for well-watered and drought environments **Plant Physiology** (submitted)

Bragg, N.B., Anderton, A., Nieu, R., and Vogel, J.P. 2015 *Brachypodium distachyon.* ***Agrobacterium*** **Protocols: Volume 1 (Methods in Molecular Biology vol. 1223)** Wang. K., New York, Springer. 2015, pp 17-33

Poiré R., Chochois V., Sirault X.R.R., Vogel J.P., Watt M., Furbank R.T., 2014 Whole plant phenotypic variability in nitrogen and phosphorus response of *Brachypodium distachyon* **Journal of Integrative Plant Biology** 56: 781-796

Tyler L., Fangel J.U., Fagerström A.D., Steinwand M.A., Raab, T.K., Willats, W.G.T., Vogel, J.P. 2014 Selection and phenotypic characterization of a core collection of *Brachypodium distachyon* inbred lines **BMC Plant Biology** 14:25 doi:10.1186/1471-2229-14-25

Catalan P, Chalhoub B, Chochois V, Garvin DF, Hasterok R, Manzaneda AJ, Mur LAJ, Pecchioni N, Rasmussen SK, Vogel JP, Voxeur A 2014 Update on the genomics and basic biology of Brachypodium. **Trends in Plant Science** 19: 414-418

Schneebeli . 2014 *Brachypodium distachyon*: a pathosystem model for the study of the wheat root disease *Rhizoctonia* root rot. **PhD Thesis. Australian National University**

Gordon, S.P., Priest, H., Des Marais, D.L., Schackwitz, W., Figueroa, M., Martin, J., Bragg, J.N., Tyler, L., Lee, C.R., Bryant, D., Wang, W., Messing, J., Manzaneda, A.J., Kerrie, B., Garvin, D.F., Budak, H., Tuna, M., Mitchell-Olds, T., Pfender, W.F., Juenger, T.E., Mockler, T.C., and Vogel, J.P., 2014 Genome Diversity in *Brachypodium distachyon*: Deep Sequencing of Highly Diverse Inbred Lines 2014 **Plant Journal** 79: 361–374 DOI: 10.1111/tpj.12569

Manuscripts close to submission, all work completed manuscripts partially written (3)

Crackle 1, a gene required for leaf integrity in the model grass *Brachypodium distachyon*, 2015 Bragg, J., Anderton, A., Nieu, Vogel, J., **Plant Physiology** (will be submitted shortly)

Bushy 1, a gene required for male fertility and normal development in *Brachypodium distachyon*, but not in *Arabidopsis thaliana* 2015 Bragg, J., Anderton, A., Nieu, Vogel, J., **Plant Journal** (will be submitted shortly)

Phenotyping systems for the root systems of the model grass *Brachypodium distachyon.* 2015 Chochois V, Dong, P, Schneebeli K, Vogel, J, Watt M ., **Plant Methods** (will be submitted shortly)

Planned manuscripts, data analysis and/or small confirmatory experiments need to be completed before the manuscripts can be written (4)

Phenomic analysis of natural diversity in the model grass *Brachypodium distachyon*, Poiré R., Chochois V., Sirault X.R.R., Bragg, J., Watt M., Vogel J.P., Furbank R.T.

Phenomic analysis of homozygous *Brachypodium distachyon* T-DNA lines. Bragg, J., Poiré R., Chochois V., Sirault X.R.R., Watt M., Furbank R.T. Vogel J.P.

Identification of QTLs for growth rate and biomass accumulation in a RIL population of *Brachypodium distachyon*. Poiré R., Sirault X.R.R., Furbank R.T. Vogel J.P.

Natural diversity of photosynthetic capacity of *Brachypodium distachyon*. Poiré R., Sirault X.R.R., Vogel J.P., Furbank R.T.

Invited presentations at scientific conferences (7)

"Phenomic analysis of natural and induced variation in *Brachypodium distachyon*" September 25, 2013, a plenary talk presented at the 15th Annual Fall Symposium: PhenoDays: Imaging and Robotics for 21st Century Science, Donald Danforth Plant Science Center, St Louis, MO

"Brachypodium: a functional and genomic model for wheat root architecture and rhizosphere interactions." June 2013, Keynote address at the First International Brachypodium Meeting, Modena, Italy.

"Phenomic characterization of Brachypodium collections and an update on community resources: T-DNA lines, resequencing, polyploidy and perenniality" February 25, 2013 a talk presented at the DOE Genomic Science Contractors-Grantees Meeting, Bethesda, MD

"Tools to study cell walls in the model grass *Brachypodium distachyon*" August 5, 2012, a plenary talk presented at the Gordon Research Conference on Plant Cell Walls, Waterville, Maine

"Emerging genomic resources for the model grass Brachypodium distachyon" a plenary talk presented at the Cold Spring Harbor Laboratory Plant Genomes – What's Next? conference, December 1, 2011, Cold Spring Harbor, NY

"Natural diversity from genomics to phenomics" a plenary talk presented at the First European *Brachypodium* Workshop, October 20, 2011, Versailles, France

"Phenotyping the shoot and root diversity of *Brachypodium distachyon* to accelerate plant biofuel breeding" Plant and Animal Genome conference, January 17, 2012, Sand Diego, CA

Invited seminars (3)

"*Brachypodium* as a Model for the Grasses: Functional Genomic Tools and their Application to Biomass Crop Improvement" a seminar presented at China Agricultural Univeristy and at the Chinese Academy of Sciences, Beijing, China

"Genomic and phenomic studies of the model grass *Brachypodium distachyon*" a seminar presented at the University of Toronto, Toronto, Canada April 27, 2012

"Development of genomic tools for the model grass *Brachypodium distachyon* and their application to biomass crop improvement" a seminar presented at the Renewall consortium project meeting, June 2, 2011, Dundee, UK

Seed distribution

We are now distributing seed for the homozygous lines when researchers order seeds for specific T-DNA lines.